

On the detection of superdiffusive behaviour in time series

Georg A. Gottwald* Ian Melbourne†

25 July 2016

Abstract

We present a new method for detecting superdiffusive behaviour and for determining rates of superdiffusion in time series data. Our method applies equally to stochastic and deterministic time series data and relies on one realisation (ie one sample path) of the process. Linear drift effects are automatically removed without any preprocessing. We show numerical results for time series constructed from *i.i.d.* α -stable random variables and from deterministic weakly chaotic maps. We compare our method with the standard method of estimating the growth rate of the mean-square displacement as well as the p -variation method.

1 Introduction

The ubiquity of normal diffusion can be understood by the Central Limit Theorem which, roughly speaking, states that an appropriately scaled sum of many independent identically distributed random variables with finite variance converges in distribution to a normally distributed random variable. Hence, the erratic motion of a grain of pollen suspended in water, as observed by the botanist Brown in 1827, can be understood as the relatively heavy grain experiencing the sum of many uncorrelated kicks of the chaotic

*School of Mathematics and Statistics, University of Sydney, Sydney 2006 NSW, Australia

†Mathematics Institute, University of Warwick, Coventry, CV4 7AL, UK

much lighter water molecules. It has become evident that Brownian motion and its associated normal diffusion is too simplistic to describe the variety of diffusion processes in complex systems. There are many situations where the Central Limit Theorem fails [1, 2, 3, 4, 5], and their fluctuations are of the so called Lévy type rather than of the Gaussian type. Whereas Gaussian processes are continuous processes with finite variance, Lévy processes (or α -stable processes) exhibit jumps of all sizes and have infinite variance.

Distilling the information relevant to anomalous diffusion from a time series is a scientific challenge. Distinguishing between normal and anomalous diffusion usually involves the analysis of the mean-square displacement which grows linearly for normal diffusion and sub-linearly or super-linearly for anomalous sub- and super-diffusion, respectively. We show numerically that estimating the asymptotic growth rate of the mean-square displacement is not an efficient method for distinguishing anomalous from normal diffusion; in finite-size time series the statistical behaviour of rare large jumps is not resolved. We therefore suggest to use lower-order moments of order $q \ll 1$ where the many well-resolved small jumps contribute more than rare large jumps.

In addition it is well known that the estimation of asymptotic growth rates often suffers from a bias caused by a non-zero mean of the observables, and requires error prone pre-processing of the data to subtract the mean or the employment of detrended fluctuation analysis [6, 7]. We propose a new method where an eventual non-zero mean is inherently removed by calculating the q 'th moments not of the process directly but by rotating the process with a deterministic periodic driver.

A different approach to detect anomalous diffusion is to employ the p -variation which recently found lots of application in successfully detecting anomalous behaviour in time series [8, 9, 10]. In the case of additive noise, however, this method has been shown to lead to inconclusive results as discussed in [11]. We compare our method with the standard method of estimating the asymptotic growth rate of the q 'th moment as well as with the method of p -variation for uncontaminated data and for data contaminated by biased additive measurement noise. We use data generated from *i.i.d.* random variables as well as from deterministic weakly chaotic maps.

The paper is structured as follows. In Section 2 we construct time series

exhibiting anomalous diffusion. In Section 3 we present numerical results of the asymptotic growth rates of the q 'th moment and show that high moments such as the mean-square displacement are not well suited to detect anomalous diffusion in a quantitative way. Section 4 briefly describes the methods to estimate the asymptotic growth rate of the low moments, including our new method, and two versions of the p -variation method. Numerical results are presented in Section 5. We conclude in Section 6 with a summary and discussion.

2 Time series data

We will apply the tests to discrete time series $\{\varphi(j)\}_{j=1,\dots,N}$ which are generated both stochastically and deterministically. To distill information about the diffusive nature of the underlying system we construct from the time series the Birkhoff sums

$$\Phi(n) = \sum_{j=0}^{n-1} \varphi(j). \quad (1)$$

In the stochastic case, we consider *i.i.d.* sequences of α -stable random variables $\varphi(j)$. Such random variables $S_\alpha(\beta, \mu, \sigma)$ are uniquely characterized by four parameters: asymmetry parameter β , location parameter μ and spread parameter σ together with α . Numerically, we generated these random variables via the method of Chambers, Mallows and Stuck [12]. In Figure 1 we show $\Phi(n)$ for $\alpha = 1.5$, $\beta = 1$, $\mu = 1$ and $\sigma = 0.1$. The linear drift in the Birkhoff sum $\Phi(n)$ caused by $\mu \neq 0$ has been subtracted by computing the sample mean for $\alpha > 1$, i.e. by considering $\varphi(j) \rightarrow \varphi(j) - (1/n) \sum_{m=0}^{n-1} \varphi(m)$. To generate the time series deterministically we employ Pomeau-Manneville intermittency maps [13]. In particular, we use the map $y_{n+1} = f(y_n)$ with $f : [0, 1] \rightarrow [0, 1]$ studied by [14]

$$f(y) = \begin{cases} y(1 + 2^z y^z), & y \in [0, \frac{1}{2}] \\ 2y - 1, & y \in [\frac{1}{2}, 1] \end{cases}. \quad (2)$$

This map has a neutral fixed point at $y = 0$. For $z = 0$ the map reduces to the doubling map which preserves the uniform measure on the interval $[0, 1]$ and exhibits exponential decay of correlations. For $z \in (0, 1)$, there exists

a unique absolutely continuous invariant ergodic probability measure, and correlations decay at the rate $n^{-(z-1-1)}$ [15]. Correlations are summable if and only if $z < \frac{1}{2}$, and in this situation the central limit theorem applies with $n^{-\frac{1}{2}}\Phi(n)$ converging in law to a normal distribution for mean zero Hölder observables φ [16]. For $z \in (\frac{1}{2}, 1)$, however, Gouëzel [3] proved that for sufficiently smooth mean zero observables $\varphi(y)$ which are non-zero at the neutral fixed point, the central limit theorem fails and instead $n^{-z} \sum_{j=0}^{n-1} \varphi(y_j)$ converges in distribution to a stable law of exponent $\alpha = 1/z$, asymmetry $\beta = \pm 1$ and mean $\mu = 0$. The jumps are produced by the orbit spending prolonged times near 0 with $\varphi \approx \varphi(0)$. In order to get better statistics, we consider the induced map, which effectively condenses the many small jumps to a single big jump. The inducing is performed by passing from the nonuniformly expanding map $f : [0, 1] \rightarrow [0, 1]$ to the uniformly expanding first return map $F = f^\tau : Y \rightarrow Y$ with $Y = [1/2, 1]$ where $\tau(y) = \inf\{n \geq 1 : f^n y \in Y\}$ is the first return time back into the set Y for $y \in Y$. Induced observables are then defined as

$$\varphi_I(y) = \sum_{\ell=0}^{\tau(y)-1} \varphi(f^\ell y), \quad (3)$$

leading to $\Phi(n) = \sum_{j=0}^{n-1} \varphi_I \circ F^j$ via iteration of this procedure.

In Figure 1 we show the time series $\Phi(n)$ for $\alpha = 1.25$ generated via the map (2) with $z = 0.8$ for an induced observable $\varphi = 1 + y_n$. The linear drift of the Birkhoff sum $\Phi(n)$ was again approximately eliminated by subtracting the sample mean.

3 Scaling behaviour of the q 'th moments

We now investigate the scaling behaviour of the q 'th moment $\mathbb{E}|\Phi(n)|^q$. Envoing ergodicity the q 'th moment is expressed by the time average

$$\mathbb{E}|\Phi(n)|^q = \lim_{N \rightarrow \infty} \frac{1}{N} \sum_{j=0}^{N-1} |\Phi(j+n) - \Phi(j)|^q. \quad (4)$$

In the case of zero-mean *i.i.d.* α -stable random variables, the q 'th moments exist for $q < \alpha$ and scale as

$$\mathbb{E}|\Phi(n)|^q \sim n^{\frac{q}{\alpha}}. \quad (5)$$

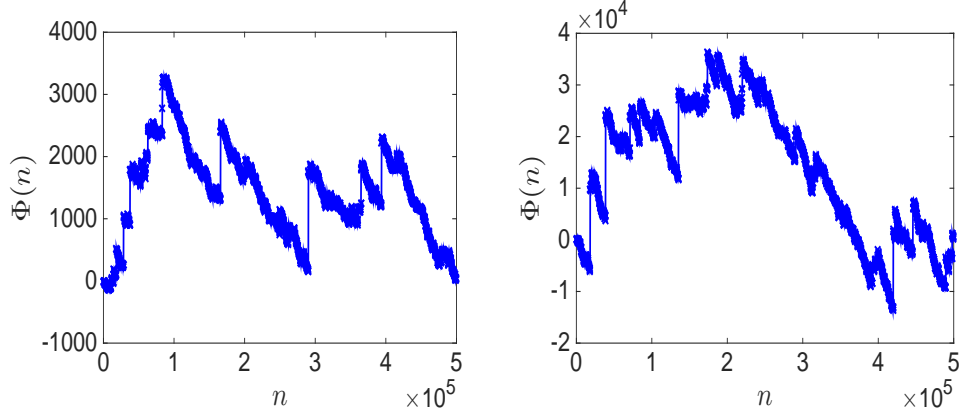


Figure 1: Realization of an α -stable process $\varphi(n)$ generated from *i.i.d.* variables with $\alpha = 1.25$, $\beta = 1$, $\mu = 1$, $\sigma = 0.1$ (left) and through the deterministic map (2) with $z = 1/1.25 = 0.8$ and observable $\varphi = 1 + x$. The sample mean has been subtracted from the observables $\varphi(j)$.

For $q \geq \alpha$ the q 'th moments do not exist. In the case of anomalous diffusion of underlying deterministic weakly chaotic dynamics, the moments exist for all values of q and scale as follows [17, 18]

$$\begin{cases} \mathbb{E}|\Phi(n)|^q \sim n^{q/\alpha} & q < \alpha \\ \mathbb{E}|\Phi(n)|^q \approx n^{q+1-\alpha} & q > \alpha \end{cases}. \quad (6)$$

(We write $a_n \sim b_n$ if there exists a constant $c > 0$ such that $\lim_{n \rightarrow \infty} a_n/b_n = c$. We write $a_n \approx b_n$ if there exists constants $C_1, C_2 > 0$ such that $C_1 \leq a_n/b_n \leq C_2$ for all $n \geq 1$.) For the Brownian motion case we obtain the linear scaling of the mean-square displacement $\mathbb{E}|\Phi(n)|^2 \approx n$.

We now investigate the scaling behaviour of the q 'th moments by plotting the growth rate

$$\gamma(q) = \lim_{n \rightarrow \infty} \frac{\log(\mathbb{E}|\Phi(n)|^q)}{\log(n)} \quad (7)$$

for several values of q for *i.i.d.* observables and from observables obtained from a deterministic intermittency map. To avoid any issue with a non-zero mean of the observables creating non-negligible drift terms of $\mathbb{E}|\Phi(n)|^q$, we

symmetrize the intermittency map (2) and consider the map $y_{n+1} = f_{\text{sym}}(y_n)$ with $f_{\text{sym}} : [-1, 1] \rightarrow [-1, 1]$

$$f_{\text{sym}}(y) = \begin{cases} -2y, & 0 \leq y \leq \frac{1}{2} \\ 1 - (1 - y)(1 + 2^z(1 - y)^z), & \frac{1}{2} \leq y \leq 1 \\ -f_{\text{sym}}(-y), & -1 \leq y \leq 1 \end{cases} \quad (8)$$

with neutral fixed points at $y = \pm 1$. To determine the asymptotic growth rate $\gamma(q)$ from a single time series, we need to respect the double limit in the temporal average (4). The double limit requires us to choose $n \ll N$. In practice we use $n \leq N/10$. The asymptotic growth rate is then determined by linear regression of $\mathbb{E}|\Phi(n)|^q$.

Figure 2 shows results of numerical simulations for time series of length $N = 500,000$. Whereas the simulations confirm the theoretical growth rate $\gamma(q)$ implied by (6) for small values of q it is clearly violated for large $q > \alpha$. In particular, for the usual value $q = 2$, the implied value for the anomalous diffusion is $\alpha_{\text{est}} = 2/\gamma \approx 2$. This suggests that the estimation of the mean-square displacement ($q = 2$) would falsely classify anomalous diffusion as normal with a linear growth.

In Figure 3 we show the q 'th moment as a function of n for several values of N for $q = 0.2$ and $q = 2$ for $\alpha = 1.25$. For $q = 0.2$, the convergence to the theoretical scaling result (5) and (6), respectively, is clearly seen (top panel). For $q = 2$, the growth rate is approximately equal to 1 for the *i.i.d.* case as well as for the Pomeau-Manneville case, consistent with the results presented in Figure 2 (bottom panel). It is also clearly seen that the 2nd moments have not converged. Note that this is consistent with the nonexistence of the 2nd moment in the *i.i.d.* case. For the deterministic Pomeau-Manneville case in which the 2nd moment exists, however, this illustrates that $N = 500,000$ is insufficient to determine the slope of $3 - \alpha$ (cf (6)).

The results show that calculating the mean-square displacement is not satisfactory for distinguishing anomalous superdiffusion and normal diffusion in finite time series; note that the time series of $N = 500,000$ data points is rather large. The results rather suggest to use lower moments with small values of q to estimate the anomalous coefficient α . A heuristic explanation for the superior performance of lower moments is that in a finite data set the statistics of the large jumps are necessarily not well resolved. For low values of $q \ll 1$ the smaller jumps, for which better statistics are available within a

finite data set, receive a relatively larger weighting than larger jumps in the time average (4). The relative importance of large jumps in the q 'th moment (4) is increased for large values of q .

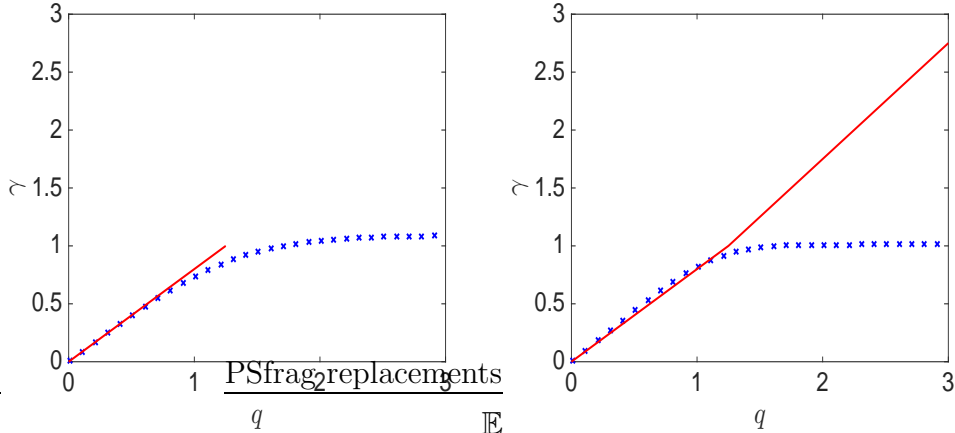


Figure 2: The growth rate γ of the q 'th moment $\mathbb{E}|\Phi|^q \sim n^\gamma$ for $\phi(x) = x$ as a function of q for the *i.i.d.* case with $\mu = 0$, $\sigma = 0.1$, $\beta = 0$ and $\alpha = 1.25$ (left) and for the Pomeau-Manneville map (8) (right) for $\alpha = 1.25$. The continuous curve (online red) depicts the theoretical result according to (5) or (6), respectively.

4 Methods of detection

4.1 Measuring the asymptotic growth rate of the q 'th moment via an \mathbb{R} -extension

The first method is the standard determination of the asymptotic growth rate γ of the q 'th moment via linear regression for a given time series of length N . Motivated by the numerical results from the previous Section we choose $q = 1/8$. We remark, that we can interpret the Birkhoff sum (1) as an \mathbb{R} -extension, driven by the time series $\varphi(j)$. A non-zero mean of the observables $\varphi(j)$ would dominate the asymptotic behaviour of the q 'th moments leading to $\gamma(q) = q$, independent of the underlying diffusive nature of the dynamics. We therefore subtract the sample mean $N^{-1} \sum_{j=0}^{N-1} \varphi(j)$ from the observables for $\alpha > 1$. Note that the mean is not defined for $\alpha < 1$ in the case of *i.i.d.*

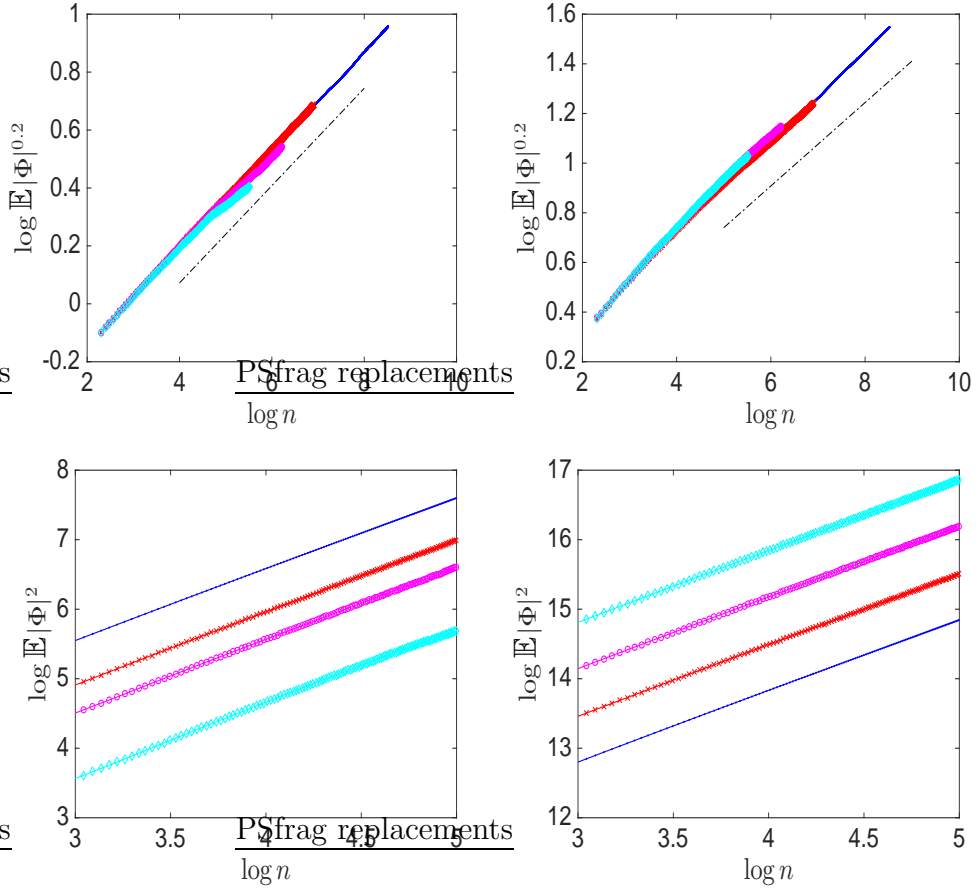


Figure 3: The q th moment $\mathbb{E}|\Phi|^q$ for $\varphi(x) = x$ for the *i.i.d.* case (left) and for the Pomeau-Manneville map (8) (right). Results are shown for $\alpha = 1.25$ for time series of length $N = 500,000$ (dashed line, online blue), $N = 100,000$ (crosses, online red), $N = 50,000$ (open circles, online magenta) and $N = 25,000$ (diamonds, online cyan). Top: For $q = 0.2 < \alpha$. Bottom: For $q = 2 > \alpha$. The dashed lines in the top figures show the theoretical slope as calculated via (5) and (6), respectively. The slope in the bottom figures is approximately 1 (cf. Figure 2).

random variables (cf. Section 3). Hence, without *a priori* knowledge of α , subtracting the sample mean is problematic.

4.2 Measuring the asymptotic growth rate of the q 'th moment via an $\mathbf{E}(2)$ -extension

To account for a possible non-zero mean of the observables $\varphi(j)$ we consider instead of (1) the following Birkhoff sum

$$\Phi_c(n) = \sum_{j=0}^{n-1} \varphi(j) \cos cj \quad (9)$$

where $c \neq 0$. Including the rotational variable $\cos cj$ assures that the mean of Φ_c is automatically zero. We will see in Section 5 that this has advantages over manually subtracting the sample mean, as in the previous Subsection, which may contaminate the statistics. We then calculate the q 'th moment $\mathbb{E}|\Phi_c|^q$ and measure its asymptotic growth rate γ_c . We will again use $q = 1/8$. Resonances between the rotational variable and the actual underlying dynamics encoded in the observable will obscure the information contained in $\gamma_c(q)$. Such resonances correspond to a term in the Fourier decomposition of the time series $\varphi(j)$ proportional to $\exp(-ick)$ leading to $\Phi(n) \sim n$ implying an asymptotic growth rate $\gamma_c = q$, independent of the actual diffusive behaviour. We therefore compute the median of γ_c over several values of c . We choose to compute the median rather than the mean to avoid the effect of outliers. In practice we find that 100 values of $c \in (\pi/5, 4\pi/5)$ are sufficient. We remark that the Birkhoff sum (9) can be viewed as an $\mathbf{E}(2)$ -group extension driven by the time-series. The inclusion of a rotational variable has proven very useful in the detection of deterministic chaos using the 0-1 test for chaos [19, 20, 21, 22].

4.3 p -variation method

The p -variation associated with a process Φ is defined as the asymptotic limit

$$V_p(t) = \lim_{n \rightarrow \infty} V_p^n(t) , \quad (10)$$

where $V_p^n(t)$ is the partial sum of increments of the observable $\Phi(n)$ given by

$$V_p^n(t) = \sum_{k=1}^{\lfloor nt \rfloor} \left| \Phi\left(\frac{k}{n}\right) - \Phi\left(\frac{k-1}{n}\right) \right|^p.$$

For $p = 1$, $V_1(t)$ reduces to the total variation, and for $p = 2$, $V_2(t)$ reduces to the quadratic variation. It is known that for Brownian motion, $V_2(t) \sim t$ and $V_p(t) = 0$ for any $p > 2$. In the case of subdiffusion, the p -variation allows to distinguish fractional Brownian motion and Continuous Time Random Walk (CTRW) diffusion [8, 9]. For fractional Brownian motion, $V_2(t) = \infty$ and $V_{2/\gamma^*}(t) \sim t$, whereas for CTRW, $V_2(t)$ is a monotonically increasing step function and $V_{2/\gamma^*}(t) = 0$, where $\gamma^* = \gamma(2)$ is the asymptotic growth rate of the mean-square displacement. For superdiffusion, $V_p^n(t)$ converges for $p > \alpha$ and diverges for $p < \alpha$ for $n \rightarrow \infty$. This suggests to estimate α by determining the smallest value p^* for which convergence occurs and set $\alpha_{\text{est}} = p^*$. In practice, we subsample a time series of length N into 2^m data points with equal spacing $N/2^m$ with $m = 0, \dots, \lfloor \log N / \log 2 \rfloor$. For the finest samplings we estimate a linear approximation $\hat{V}_p^n(t)$ by linear regression of $V_p^n(t)$. We determine p^* then as the minimal value of p for which the ℓ_1 -norm of the difference between two consecutive samplings $|\hat{V}_p^n(t) - \hat{V}_p^{n-1}(t)|$ falls below some threshold θ_p . The choice of the threshold θ_p is, of course, arbitrary and depends on the underlying dynamical system which is analyzed.

4.4 Modified p -variation method

In [23, 10] theorems were proved showing that for an α -stable random variable with location parameter $\mu = 0$ and $\alpha = p/2$ (and any values of β and σ) its p -variation $V_p^n(t)$ converges in distribution to an $\alpha = 1/2$ -stable random variable $S_{1/2}(1, 0, \sigma)$ with some specified spread parameter σ . In [10] this was developed into a time series analysis method using a Kolmogorov-Smirnov test and finding the value of $p = 2\alpha$ for which the empirical cumulative distribution function is closest to the target cumulative distribution function of $S_{1/2}(1, 0, \sigma)$. To estimate the cumulative distribution function of $V_p^n(t)$, an ensemble of p -variations is generated by segmenting the time series into M pieces, each being $\lfloor N/M \rfloor$ long. This tacitly assumes that the samples are uncorrelated which is only approximately true for sufficiently long segments in the deterministic case. The minimal Kolmogorov-Smirnov distance is determined by varying the spread parameter σ of the target distribution

$S_{1/2}(1, 0, \sigma)$ for each value of p . The value p^* for which the minimum is attained then determines $\alpha = p^*/2$. The precise mathematical statement is provided in A. For details on the modified p -variation method see [23, 10].

5 Numerical results

We use a time series of length $N = 25,000$ calculated from *i.i.d.* random variables and from weakly chaotic deterministic variables. We will show results for pure data and for noise-contaminated data. To calculate the q 'th moments $\mathbb{E}|\Phi|^q$ we will employ $q = 1/8$. For the p -variation method we use $\theta_p = 0.01$ and cycle through p in increments of $\Delta p = 0.005$. We found that larger values of θ_p will perform better for larger values of α but worse for smaller values of α . For the modified p -variation method, we choose $M = 250$ samples of length 100 each, and cycle through 10,000 values of the spread parameter $\sigma \in (10^{-2}, 10^{10})$ (equidistant in log-space).

5.1 Results for the *i.i.d.* case

We use a time series of length $N = 25,000$ constructed by the Chambers, Mallows and Stuck [12] method. We set the asymmetry parameter $\beta = 1$ and the spread parameter $\sigma = 0.1$, and allow for a non-zero mean parameter $\mu = 2$.

In Figure 4 we show results for the estimated value of α for all four methods described in the previous Section. For the methods using the asymptotic growth rate γ we estimate the implied value for $\alpha_{\text{est}} = q/\gamma$ for $\alpha > q$. The method of estimating α via the asymptotic growth rate of the q 'th moment using the \mathbb{R} -extension method performs very well for $\alpha < 1$, but has large errors for $\alpha > 1$. This is due to the non-accuracy in determining the mean via the sample mean which is subtracted for $\alpha > 1$. This undesirable property is alleviated when estimating the asymptotic growth rate of the q 'th moment from an $\mathbf{E}(2)$ -extension, where α is well estimated for the whole range of α . The standard p -variation performs well except near $\alpha = 1$ and $\alpha = 2$. It is more accurate than the $\mathbf{E}(2)$ -method for $1 < \alpha < 1.5$. The modified p -variation has strong difficulties in estimating the anomalous diffusion near $\alpha = 1$ and $\alpha > 1.75$. We have tested that the bad performance of the modified p -variation method near $\alpha = 1$ is due to the non-vanishing mean parameter $\mu = 2$ and the asymmetry $\beta = 1$. For $\mu = 0$ and $\beta = 0$ (and all

other parameters unchanged), the modified p -variation method performs well near $\alpha = 1$. The bad performance near the Brownian case $\alpha = 2$ remains though for $\mu = 0$ and $\beta = 0$.

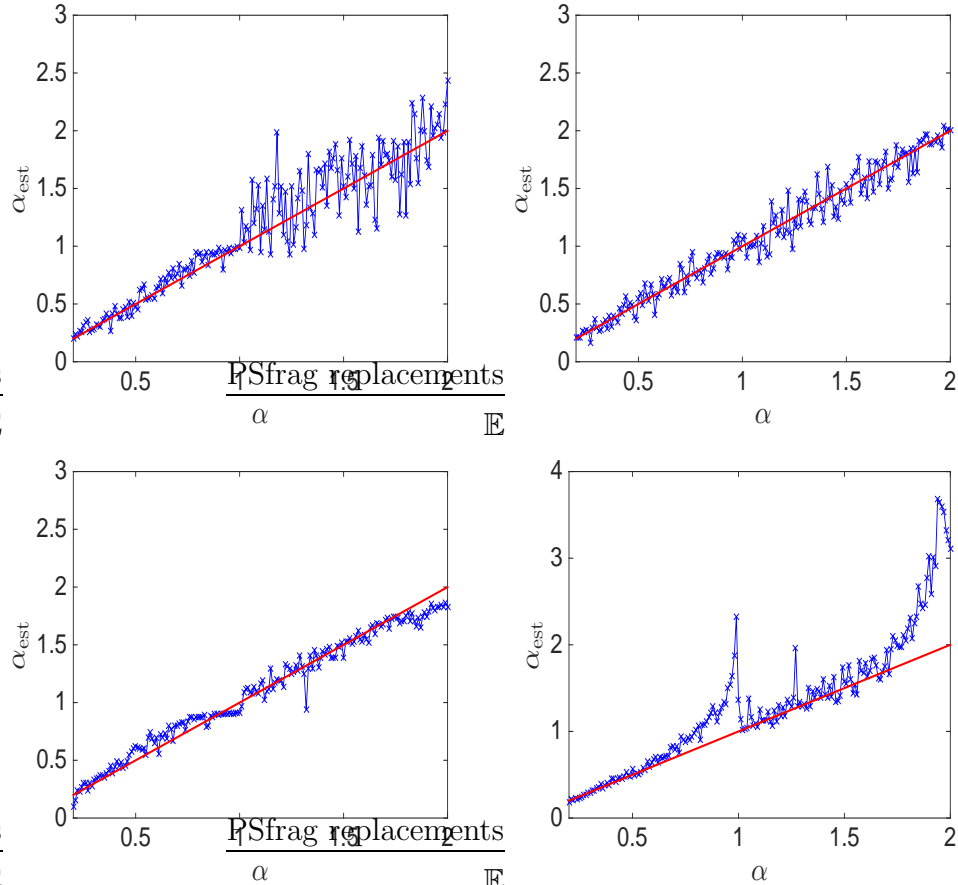


Figure 4: Estimates α_{est} as calculated for several values $\alpha \in (0.2, 2)$ for *i.i.d.* observations. Top left: method of q 'th moment from \mathbb{R} -extension with $q = 1/8$. Top right: method of q 'th moment from $\mathbf{E}(2)$ -extension with $q = 1/8$. Bottom left: p -variation method. Bottom right: modified p -variation method (note the larger range on the y -axis).

We also present results where we contaminate the observations $\varphi(n)$ by biased uniform noise according to $\varphi(n) \rightarrow (1 + \eta u)\varphi(n)$ with $u \sim U(0, 1)$ in Figure 5. We choose here relatively large additive measurement noise with

$\eta = 0.5$. The additive noise makes detection more difficult for determining the asymptotic growth rate of the q 'th moment but much less so if the $\mathbf{E}(2)$ -extension is used. The standard p -variation also becomes less reliable for $1 < \alpha < 2$ when additive noise is included, consistent with the results reported in [11]. The modified p -variation exhibits some deteriorating sensitivity to additive noise.

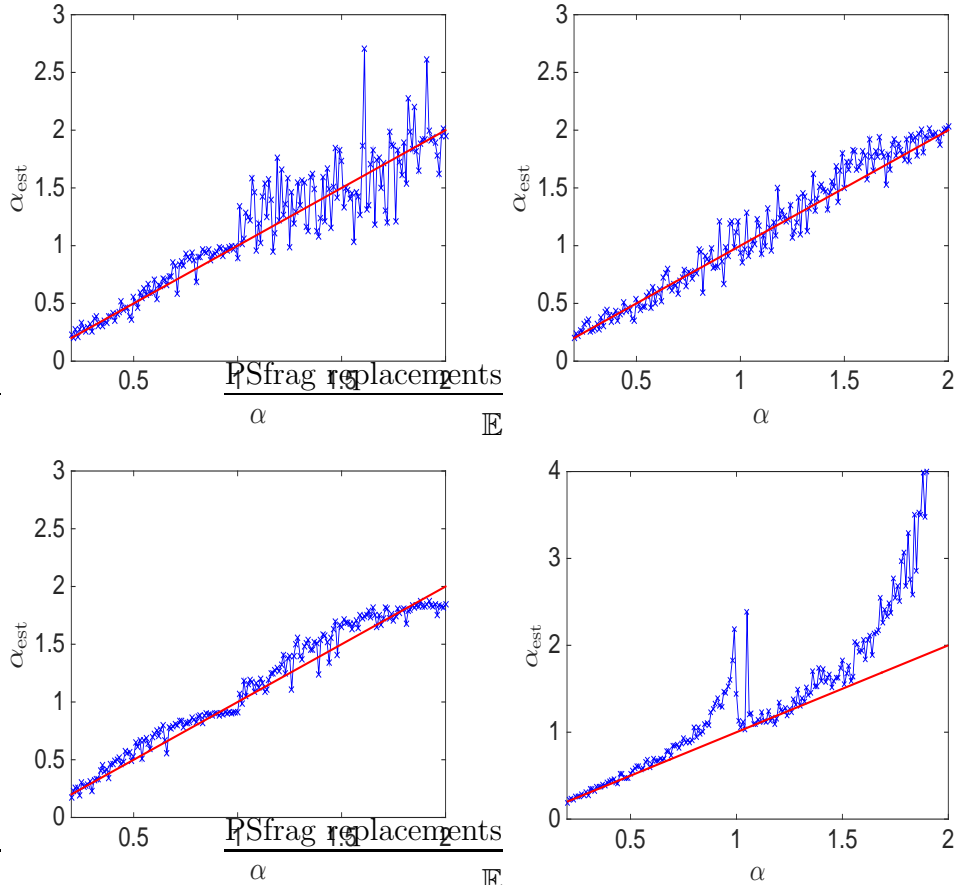


Figure 5: Estimates α_{est} as calculated for several values $\alpha \in (0.2, 2)$ for *i.i.d.* observations with 50% biased measurement noise. Top left: method of q 'th moment from \mathbb{R} -extension with $q = 1/8$. Top right: method of q 'th moment from $\mathbf{E}(2)$ -extension with $q = 1/8$. Bottom left: p -variation method. Bottom right: modified p -variation method (note the larger range on the y -axis).

5.2 Results for the Pomeau-Manneville case

We use a time series of length $N = 25,000$ constructed from the Pomeau-Manneville map (2) for $\alpha \in (0.6, 2)$. We choose $\varphi(n) = 1 + x_n$. Figure 6 shows the analogous results to Figure 4.

In the deterministic case, we observe the same behaviour of the \mathbb{R} -extension method as in the *i.i.d.* case where anomalous diffusion is very well classified for $\alpha < 1$ but not so well for $\alpha > 1$ where the error in estimating the sample mean has a detrimental effect. The **E(2)**-method performs well, except near the Brownian case of $\alpha = 2$ where it underestimates the anomalous scaling coefficient. The slow convergence may be related to cross-correlation effects that arise in the diffusion parameter via the Green-Kubo formula. Such cross-correlations are not present in the superdiffusive case $\alpha < 2$ [3]. The p -variation also does not perform well. Near $\alpha = 1$ and the Brownian case $\alpha = 2$ the p -variation strongly flattens and underestimates the anomalous scaling coefficient. The modified p -variation, in contrast, performs well for the whole range of α .

Again, we also present results for observations which have been contaminated with biased uniform noise with $\eta = 0.5$ in Figure 7. As in the *i.i.d.* case, the performance of the \mathbb{R} -extension method and the p -variation method is diminished by the additive measurement noise. The performance of the **E(2)** method and the modified p -variation method, however, are robust against additive measurement noise.

6 Summary and Discussion

We have introduced a new method to quantitatively estimate the degree of anomalous superdiffusion. Our method uses the asymptotic growth rate of a low-order moment of the process rotated with a periodic deterministic signal, a so-called **E(2)**-extension.

We established that the standard method of estimating the growth-rate of the mean-square displacement is not able to reliably distinguish superdiffusion from normal diffusion in finite time series. We have compared our method then with three other methods, an \mathbb{R} -extension for low order moments as well as two versions of the p -variation method.

Our numerical simulations on *i.i.d.* data and data generated deterministically from weakly chaotic Pomeau-Manneville maps, reveal that our new method

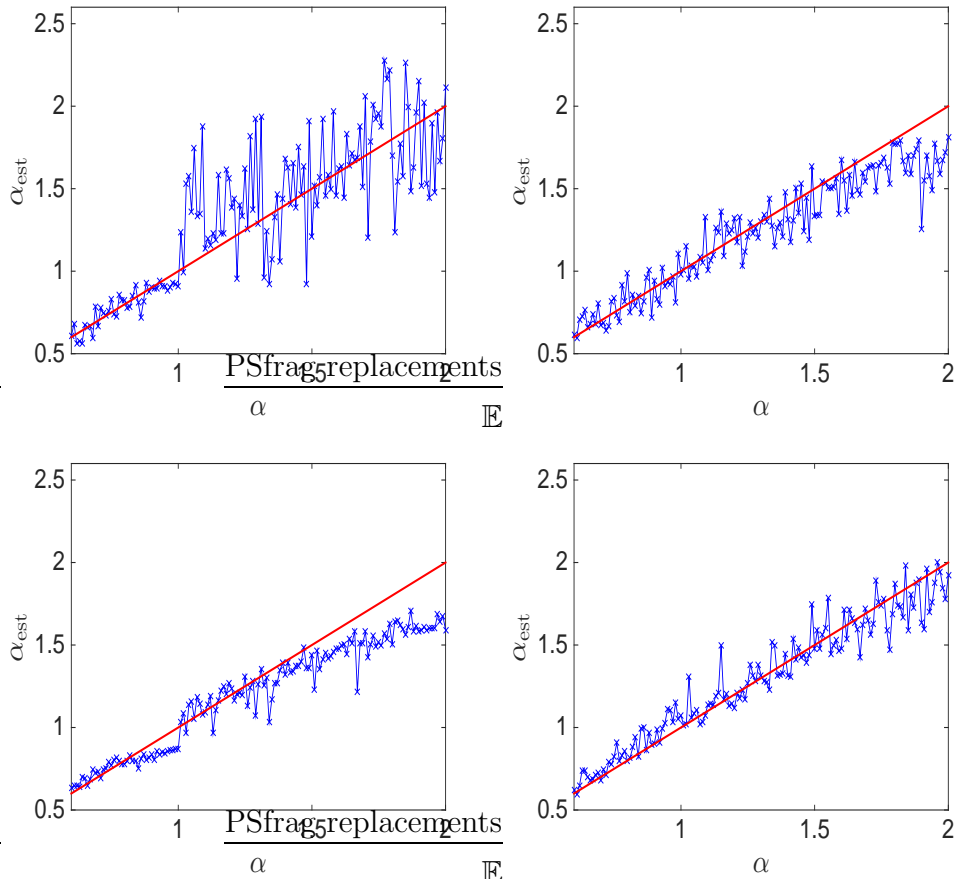


Figure 6: Estimates α_{est} as calculated for several values $\alpha \in (0.6, 2)$ for the Pomeau-Manneville map (2). Top left: method of q 'th moment from \mathbb{R} -extension with $q = 1/8$. Top right: method of q 'th moment from $\mathbf{E}(2)$ -extension with $q = 1/8$. Bottom left: p -variation method. Bottom right: modified p -variation method.

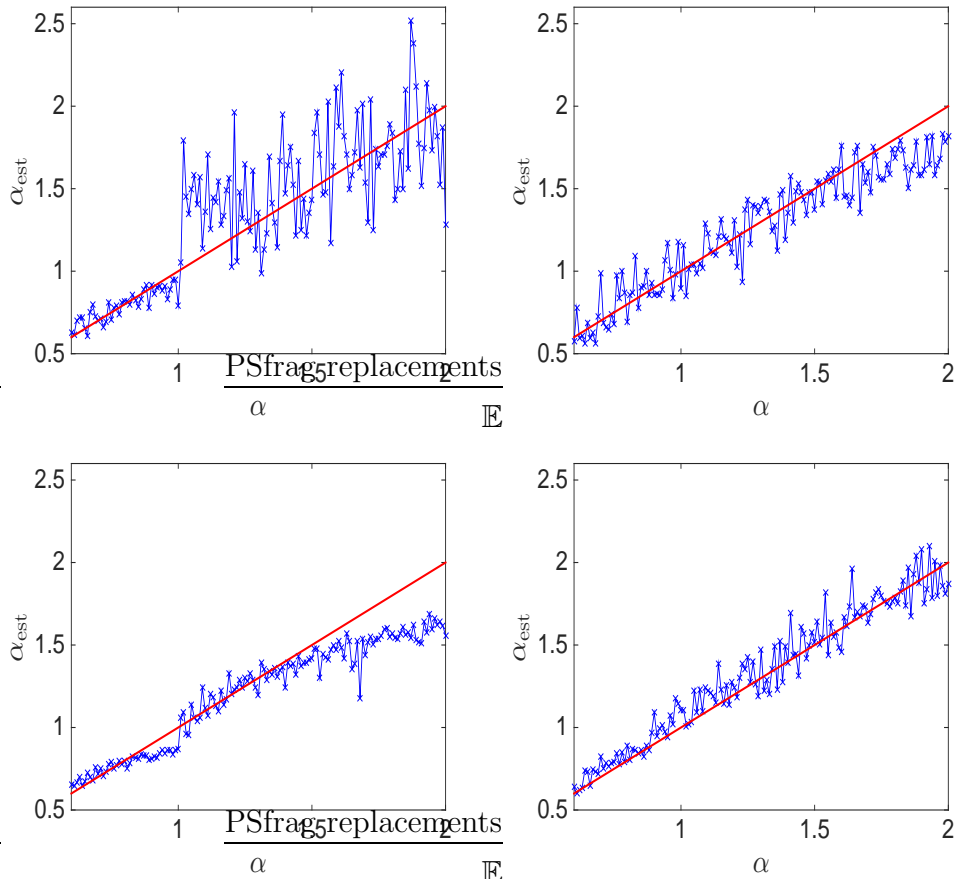


Figure 7: Estimates α_{est} as calculated for several values $\alpha \in (0.6, 2)$ for the Pomeau-Manneville map (2) with 50% biased measurement noise. Top left: method of q 'th moment from \mathbb{R} -extension with $q = 1/8$. Top right: method of q 'th moment from $\mathbf{E}(2)$ -extension with $q = 1/8$. Bottom left: p -variation method. Bottom right: modified p -variation method.

and the modified p -variation as proposed in [10] perform best and are most robust to additive measurement noise, which is inevitable in any real-world application. The modified p -variation and our newly proposed **E(2)**-method have been shown to have complementary advantages. Whereas the modified p -variation performs very well in the case of deterministic data, it did less so for the *i.i.d.* case, in particular for values of α near 1 and 2. In contrast, the **E(2)**-method performs well in the case of *i.i.d.* random variables, but becomes less accurate in the deterministic case for values of α approaching Brownian diffusion with $\alpha = 2$. We therefore propose our method to be used in conjunction with the p -variation to gain further insights into the quantitative analysis of anomalous diffusion from time series.

The computational cost involved in applying those methods varies significantly. The standard p -variation method and the \mathbb{R} -extension method of estimating the asymptotic growth rate of a low-order q 'th moment are the least computationally demanding methods. In the **E(2)**-extension method, one needs to cycle over typically 100 different values of the frequency c of the periodic signal. The modified p -variation method requires cycling through values of σ , which requires tuning over a large range of values. Despite the variation in the computational cost of the methods, all the methods use only a single sample time series.

Acknowledgements This research was supported in part by an International Research Collaboration Award at the University of Sydney. The research of IM was supported in part by a European Advanced Grant StochExtHomog (ERC AdG 320977).

A Modified p -variation

We recall here Theorem 2.1 from [10]

Theorem 1 *For an α -stable process X_t with $X_t \sim S_\alpha(\beta, 0, \sigma)$, we have for $p > \alpha/2$ that its p -variation $V_p^n(t)$ converges in the Skorohod topology with*

$$V_p^n(t) - ntB_n(\alpha, p) \xrightarrow{\mathcal{D}} X'_t \text{ as } n \rightarrow \infty,$$

where $X'_t \sim S_{\frac{\alpha}{p}}(1, 0, \sigma')$ with spread parameter

$$\sigma' = \begin{cases} \sigma^p \left(\frac{\cos(\frac{\pi\alpha}{2p})\Gamma(1-\frac{\alpha}{p})}{\cos(\frac{\pi\alpha}{2p})\Gamma(1-\alpha)} \right)^{p/\alpha} & \alpha \neq p \\ \sigma & \alpha = p \end{cases}, \quad (11)$$

and normalising sequence

$$B_n(\alpha, p) = \begin{cases} n^{-p/\alpha} \mathbf{E}|X|^p & p \in (\alpha/2, \alpha) \\ \mathbf{E} \sin(n^{-1}|X|^\alpha) & \alpha = p \\ 0 & p > \alpha \end{cases} . \quad (12)$$

References

References

- [1] Klafter J, Shlesinger M and Zumofen G 1996 *Physics Today* **49** 33
- [2] Gaspard P and Wang X J 1988 *Proceedings of the National Academy of Sciences* **85** 4591–4595
- [3] Gouëzel S 2004 *Probability Theory and Related Fields* **128** 82–122
- [4] Cont R and Tankov P 2004 *Financial modelling with jump processes* Chapman & Hall/CRC Financial Mathematics Series (Chapman & Hall/CRC, Boca Raton, FL)
- [5] Mantegna R N and Stanley H E 2007 *An introduction to econophysics: correlations and complexity in finance* (Cambridge University Press, Cambridge).
- [6] Peng C K, Buldyrev S V, Havlin S, Simons M, Stanley H E and Goldberger A L 1994 *Phys. Rev. E* **49**(2) 1685–1689
- [7] Peng C K, Havlin S, Stanley H E and Goldberger A L 1995 *Chaos* **5** 82–87
- [8] Magdziarz M, Weron A, Burnecki K and Klafter J 2009 *Phys. Rev. Lett.* **103**(18) 180602

- [9] Magdziarz M and Klafter J 2010 *Phys. Rev. E* **82**(1) 011129
- [10] Hein C, Imkeller P and Pavlyukevich I 2009 Limit theorems for p -variations of solutions of SDEs driven by additive stable Lévy noise and model selection for paleo-climatic data *Recent Development in Stochastic Dynamics and Stochastic Analysis (Interdisciplinary Math. Sciences* vol 8) ed Duan J, Luo S and Wang C (World Scientific, Singapore) pp 137–150
- [11] Jeon J H, Barkai E and Metzler R 2013 *The Journal of Chemical Physics* **139** 121916
- [12] Chambers J M, Mallows C L and Stuck B W 1976 *Journal of the American Statistical Association* **71** pp. 340–344
- [13] Pomeau Y and Manneville P 1980 *Comm. Math. Phys.* **74** 189–197
- [14] Liverani C, Saussol B and Vaienti S 1999 *Ergodic Theory Dynam. Systems* **19** 671–685
- [15] Hu H 2004 *Ergodic Theory Dynam. Systems* **24** 495–524
- [16] Young L S 1999 *Israel Journal of Mathematics* **110** 153–188
- [17] Gouëzel S and Melbourne I 2014 *Electron. J. Probab.* **19** no. 93, 30
- [18] Dedecker J and Merlevède F 2015 *Stochastic Process. Appl.* **125** 3401–3429
- [19] Gottwald G A and Melbourne I 2004 *Proc. Roy. Soc. A* **460** 603–611
- [20] Gottwald G A and Melbourne I 2005 *Physica D* **212** 100–110
- [21] Gottwald G A and Melbourne I 2009 *Nonlinearity* **22** 1367–1382
- [22] Gottwald G A and Melbourne I 2009 *SIAM J. Appl. Dyn.* **8** 129–145
- [23] Corcuera J M, Nualart D and Woerner J H C 2007 *Stochastic Analysis and Applications* **25** 169–186